



Selective hydrogenation of nitrocyclohexane to cyclohexanone oxime by alumina-supported gold cluster catalysts

Ken-ichi Shimizu^{a,*}, Takumi Yamamoto^b, Yutaka Tai^c, Atsushi Satsuma^b

^a Catalysis Research Center, Hokkaido University, N-21, W-10, Sapporo 001-0021, Japan

^b Department of Molecular Design and Engineering, Graduate School of Engineering, Nagoya University, Nagoya 464-8603, Japan

^c Materials Research Institute for Sustainable Development, Chubu Research Base of National Institute of Advanced Industrial Science and Technology (AIST), Nagoya 463-8560, Japan

ARTICLE INFO

Article history:

Received 8 December 2010

Received in revised form 12 May 2011

Accepted 21 May 2011

Available online 27 May 2011

Keywords:

Selective hydrogenation

Gold catalysts

Cyclohexanone oxime

ABSTRACT

Metal oxides (Al_2O_3 , SiO_2 , MgO)-supported Au cluster catalysts prepared by colloid deposition method and well established Au/ TiO_2 prepared by deposition–precipitation method were tested for the selective reduction of nitrocyclohexane into cyclohexanone oxime. The activity and selectivity depended strongly on the size of Au and support material. Au/ Al_2O_3 with smaller Au particle size (2.5 nm) was the most effective catalyst, exhibiting a high cyclohexanone oxime yield (86%) under mild condition (0.6 MPa H_2 , 100 °C). To study the origin of support and size effects, in situ FTIR experiments for OH/ D_2 exchange reaction and nitrobenzene adsorption combined with poisoning experiments using pyridine and acetic acid were carried out. It is suggested that cooperation of coordinatively unsaturated Au atoms and the acid–base pair site ($\text{Al}^{\delta+}-\text{O}^{\delta-}$ site) plays an important role in H_2 dissociation step. $\text{Al}^{\delta+}-\text{O}^{\delta-}$ site also acts as the adsorption site of the nitro group.

© 2011 Elsevier B.V. All rights reserved.

1. Introduction

Since Haruta discovered a remarkable activity of supported gold nanoparticles (NPs) in CO oxidation, many publications have been devoted to clarify the factors controlling the activity of gold catalysts [1–6]. Among them the most relevant appears to be particle size, the nature of the support and preparation method. For many catalytic systems, including oxidation and hydrogenation reactions, there is a general tendency that Au NPs on inert oxides, such as SiO_2 and Al_2O_3 , exhibit lower activity for various reactions than those on reducible semiconductor oxides, such as TiO_2 [1,3,7], and it is widely believed that this tendency is due to the oxygen vacancies at metal support interface of Au/ TiO_2 . The low activity of Au NPs on inert oxides should be partly due to a difficulty in controlling the size and oxidation state of gold using the conventional deposition–precipitation method. For example, when Al_2O_3 -supported gold catalysts are prepared by the deposition–precipitation method, small Au NPs (2–3 nm) as major species, larger Au particles (4.3–20 nm) [5,6] and slightly oxidized gold species [5] coexist on the support, and such non-uniform structural features can lead to lower catalytic activity. Recently, one of the authors [8] has reported that the colloid deposition method allows dispersion of metallic gold NPs with a narrow size distribution on various supports, including inert oxides such as SiO_2 .

Adopting this method, we have recently investigated the support effect of Au cluster catalysts for the selective hydrogenation of nitro group in the presence of other reducible functional groups and found that small Au clusters supported on a non-reducible support, Al_2O_3 , gave the highest activity and selectivity [9]. Based on the fundamental studies, we proposed that cooperation of the acid–base pair site on Al_2O_3 and the coordinatively unsaturated Au atoms on Au clusters is responsible for the rate-limiting H_2 dissociation to yield a H^+/H^- pair at metal/support interface. Theoretical and experimental studies established that dissociative chemisorption of H_2 does not occur on clean gold extended surfaces but can occur on low coordinated Au atoms at corners or edges of Au NPs [10–13]. Based on these backgrounds, it is of fundamental importance to expand the applicability of our hypothesis to other Au-catalyzed hydrogenation reactions.

The production of cyclohexanone oxime is an important step in the production of nylon-6. The methods presently employed in the manufacture of cyclohexanone oxime cannot avoid the production of ammonium sulfate and the use of hazardous chemicals such as oleum, halides and nitrogen oxides. There have been many attempts to change the process into environmentally benign ones [14–18]. Considering recent advances in the selective nitration of cyclohexane to nitrocyclohexane [19,20], one step hydrogenation of nitrocyclohexane into cyclohexanone oxime can be one of the alternative methods [16,17]. However, previous examples, salts of Cu(II) and Ag(I) as homogeneous catalysts [17] and a supported Pd catalyst [16], have drawbacks such as high pressures (35 bar) and the formation of environmentally unfriendly inorganic wastes.

* Corresponding author.

E-mail address: kshimizu@cat.hokudai.ac.jp (K.-i. Shimizu).

Recently, Serna et al. [18] have developed a TiO_x -decorated Pt NPs catalyst with Na-doping, which is effective for the selective hydrogenation of nitrocyclohexane to cyclohexanone oxime under mild hydrogenation conditions (4 bar of H_2). Design of alternative catalysts without the additives and platinum-group metals, such as gold catalysts, is a fundamentally more challenging target. However, a well-established Au/ TiO_2 catalyst was shown to be ineffective for this reaction [18].

Herein, we report that small Au clusters on Al_2O_3 , prepared by the colloid deposition method, catalyze the selective hydrogenation of nitrocyclohexane into cyclohexanone oxime. To establish a design concept of Au-based selective hydrogenation catalysts, we show structural studies that address the influence of the particle size and support material on catalytic efficiencies.

2. Experimental

2.1. Catalyst preparation

The TiO_2 -supported Au catalyst synthesized by a deposition–precipitation procedure (Au = 1.5 wt%, average Au particle size = 3.6 ± 0.28 nm) was purchased from the World Gold Council and was named Au/ Ti_{WGC} -3.6. γ - Al_2O_3 with surface area (S_{BET}) of $224 \text{ m}^2 \text{ g}^{-1}$ was prepared by calcination of γ - AlOOH (Catapal B Alumina purchased from Sasol) at 600°C for 3 h.

Au NPs supported on various supports (Al_2O_3 , SiO_2 , MgO) were prepared by the colloid deposition method [8]. The method we used to prepare Au NPs is the well-known two phase reduction method developed by Schiffrin and co-workers [21]. In a typical preparation of Au NPs, AuCl_4^- ions were extracted from the water into the toluene phase by excess tetraoctylammonium bromide (TOAB). After separating the toluene phase, the protecting agent dodecanethiol (DDT, Au/DDT = 1:1 mol mol $^{-1}$) was added to it at 40°C under vigorous stirring. The obtained solution was then left under stirring for 30 min. A following rapid injection of an aqueous solution of NaBH_4 (Wako, 95% purity, Au/ NaBH_4 = 1:10 mol mol $^{-1}$), led to formation of a dark orange–brown solution, indicating the formation of the gold sol. Au cations are reduced at the boundary of the water and toluene phases. This method is advantageous in that unreacted NaBH_4 and other water-soluble byproducts such as Na^+ , Cl^- and borates can be separated from Au NPs quite easily. Transmission electron microscopy (TEM) analysis showed that the mean particle diameter of Au NPs thus prepared was 2.3 ± 0.41 nm. The support was then added to the colloidal gold solution under stirring and kept in contact until total adsorption (1 wt% of gold on the support) occurred, indicated by decoloration of the solution. The solids were collected by filtration followed by washing the solids with toluene to remove all the soluble species. The resulting composites were dried at room temperature and calcined at 300°C for 4 h under air for the combustion of thiols [8]. Al_2O_3 -supported Au NPs catalysts are designated as Au/Al- x , where x is the mean size of Au NPs (nm) estimated in our previous study. For Al_2O_3 , gold colloid with larger mean diameters (5.9 ± 0.49 nm) prepared through annealing the mixture of as-prepared Au NPs and TOAB at 165°C was used, and the prepared catalyst was named Au/Al-6.0. The sample named Au/Al-30, composed of large gold particles (30 nm), was prepared by calcining the Au/Al-2.5 sample at 1000°C for 3 h. Preparation methods and structural characteristics of the catalysts are listed in Table 1.

Al_2O_3 -supported Pt catalyst (Pt/Al-1.3, Pt = 1 wt%) was prepared by impregnating γ - Al_2O_3 with an aqueous HNO_3 solution of $\text{Pt}(\text{NH}_3)_2(\text{NO}_3)_2$, followed by drying at 80°C for 12 h, calcining at 500°C for 2 h, and reducing at 300°C for 0.5 h in H_2 . The average particle size of Pt (1.3 nm) was estimated with the CO uptake of the

Pt/ Al_2O_3 -1.3 sample at 25°C using the pulse-adsorption of CO in a flow of He.

2.2. In situ FTIR

In situ FTIR spectra were recorded on a JASCO FT/IR-620 equipped with a quartz IR cell connected to a conventional flow reaction system. The sample was pressed into a 20 mg of self-supporting wafer and mounted into the quartz IR cell with CaF_2 windows. Spectra were measured accumulating 5–20 scans at a resolution of 4 cm^{-1} . A reference spectrum of the catalyst wafer in He taken at measurement temperature was subtracted from each spectrum. Prior to each experiment the catalyst disk was heated in He flow ($100 \text{ cm}^3 \text{ min}^{-1}$) at 300°C for 0.5 h, followed by cooling to the desired temperature under He flow. For the introduction of organic compounds to the IR disc, the liquid compound was injected under the He flow preheated at 150°C which was fed to the in situ IR cell. Then, the IR disk was purged with He for 600 s.

2.3. Typical procedures for the catalytic test

Commercially available organic compounds were used without further purification. As-received or as-prepared catalysts were used in catalytic experiments without any pre-treatments. Catalytic experiments were carried out in a 30 cm^3 autoclave with a glass tube inside equipped with magnetic stirring. For hydrogenation of nitrocyclohexane, 0.5 mmol of nitrocyclohexane (from Tokyo Chemical Industry Co., Ltd. with purities above 95%), EtOH (1.5 cm^3) as solvent, and catalyst (Au = 0.25 mol%) were placed into the autoclave. After being sealed, the reactors were flushed with H_2 and then pressurized at 0.6 MPa, and then heated to the required temperature (typically 100°C). Conversion and yields of products were determined by GC (GC-14B, Shimadzu) with DB-1 capillary column (Shimadzu) using n -dodecane as an internal standard. The products were identified by gas chromatography/mass spectrometry (GCMS-QP5000, Shimadzu) equipped with the same column and in the same conditions as GC and also by comparison with commercially pure products. For hydrogenation of nitrobenzene, 3.0 mmol of nitrobenzene in EtOH (1.5 cm^3) with Au catalyst (Au = 0.1 mol%) were heated at 110°C for 2 h.

3. Results and discussion

3.1. Catalytic properties

Time-conversion profiles for the nitrocyclohexane hydrogenation with Au/Al-2.5, Au/Ti-3.6, and Pt/Al-1.3 are compared in Fig. 1. Recently, Serna et al. [18] showed that hydrogenation of nitrocyclohexane by H_2 over Pt/ Al_2O_3 and Pd/C, as conventional hydrogenation catalysts, results in non-selective reduction to cyclohexylamine rather than selective reduction to cyclohexanone oxime. We tested this reaction with a conventional Pt/ Al_2O_3 catalyst (Pt/Al-1.3). As shown in Fig. 1C, the undesirable byproduct (cyclohexylamine, **3**) was selectively produced by Pt/Al-1.3. After 3 h, where the conversion reached 100%, the selectivity of cyclohexanone oxime (**2**) was only 1%. Cyclohexanone (**4**), initially appeared as an unstable product, disappeared after 1 h, and then the selectivity of dicyclohexylamine (**6**) increased. Based on kinetic studies, Serna et al. [18] proposed a general reaction scheme for the metal-catalyzed hydrogenation of nitrocyclohexane. Assuming that this model is applicable in our system, a tentative reaction scheme is shown in Scheme 1, which will be verified hereafter. The results in Fig. 1C can be explained by this scheme, in which the reaction of cyclohexylamine (**3**) and cyclohexanone (**4**) under H_2 yields dicyclohexylamine (**6**). As shown in Fig. 1B, a well-established Au nanoparticle catalyst, TiO_2 -supported

Table 1
List of the catalysts.

Catalysts-x ^a	Supports	D_{NP} (nm) ^b	M (wt%)	Preparation method	T_{cal} (°C) ^c
Au/Al-2.5	γ -Al ₂ O ₃	2.3	1	Colloid deposition	300
Au/Al-6.0	γ -Al ₂ O ₃	5.9	1	Colloid deposition	300
Au/Al-30	γ -Al ₂ O ₃	2.3	1	Colloid deposition	1000
Au/Si-1.9	SiO ₂	2.3	2.5	Colloid deposition	300
Au/Mg-3.0	MgO	2.3	1	Colloid deposition	300
Au/Ti-3.6 ^d	TiO ₂ (anatase)	–	1.5	Deposition-precipitation	–
Pt/Al-1.3	γ -Al ₂ O ₃	–	1	Impregnation	500

^a Average particle size (nm) of metallic Au species estimated from the EXAFS except for Au/Al-6.0 (TEM), Au/Al-30 (XRD), Au/TiWCC-3.6 (from WGC) and Pt/Al-1.3 (CO adsorption).

^b Mean diameter of gold NPs in gold colloid used for catalyst preparation.

^c Calcination temperature.

^d Standard catalyst supplied from WGC.

Au (Au/Ti-3.6) was not suitable catalyst. After 12 h, where the conversion reached 100%, the selectivity of cyclohexanone oxime (**2**) was only 9%. Initially, cyclohexylamine (**3**), cyclohexanone (**4**), and cyclohexyl-cyclohexylidene amine (**5**) were main products. However, with an increase in the reaction time, the selectivities to these products and mass balance decreased. This indicates that these compound are unstable in the reaction condition and will be converted to GC-undetectable side products. In contrast, cyclohexanone oxime was selectively produced by the Au/Al-2.5 catalyst. After 12 h, the yield of cyclohexanone oxime reached 83% and small amount (6.8% yield) of cyclohexanone (**4**) was observed as byproduct.

Fig. 2 shows the effect of reaction conditions on the catalytic properties of Au/Al-2.5 for nitrocyclohexane hydrogenation. Fig. 2A shows the conversion and selectivities at the reaction time of 12 h as a function of the reaction temperature. Up to 100 °C, where the conversion reached 100%, the selectivities to cyclohexanone oxime (**2**) and cyclohexanone (**4**) increased with temperature, and they decreased at higher temperature. Simultaneously, cyclohexylamine (**3**), cyclohexyl-cyclohexylidene amine

(**5**), and dicyclohexylamine (**6**) appeared as by-products. The selectivity pattern is consistent with Scheme 1, where cyclohexylamine (**3**) and cyclohexanone (**4**), produced by hydrogenation and hydrolysis of cyclohexanone oxime (**2**), undergo condensation to yield cyclohexyl-cyclohexylidene amine (**5**), which will be hydrogenated to give dicyclohexylamine (**6**). Fig. 2B shows the conversion and selectivities at 100 °C after 12 h as a function of the initial H₂ pressure. No reaction occurred under the normal pressure. Increase in the H₂ pressure from 0.1 MPa to 0.6 MPa resulted in a drastic increase in the conversion (from 0% to 100%), which suggests that H₂ activation is the rate-limiting step of the present reaction. Above 0.6 MPa, the selectivity to cyclohexanone oxime (**2**) decreased, and the selectivity to cyclohexanone (**4**) was maximum at 1.1 MPa. At higher pressure, the selectivity to cyclohexanone (**4**) decreased, and cyclohexyl-cyclohexylidene amine (**5**) and dicyclohexylamine (**6**) appeared. This selectivity pattern is again consistent with Scheme 1. From these results in Figs. 1 and 2, we could conclude that Scheme 1 is a general reaction scheme for the hydrogenation of nitrocyclohexane. As for the catalytic performance, Au/Al-2.5 shows, under the optimized reaction condition ($T = 100$ °C, $t = 12$ h,

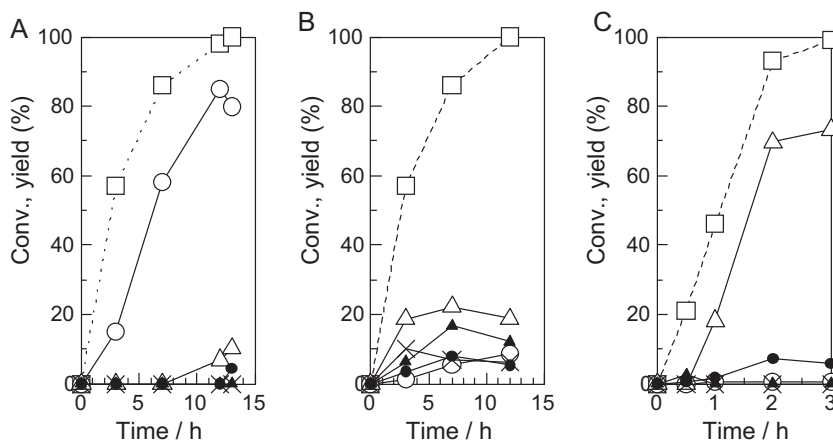
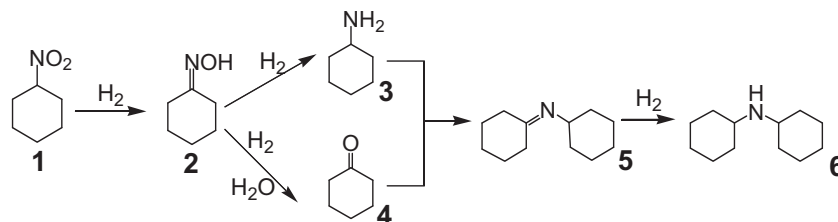


Fig. 1. Conversion of nitrocyclohexane (**1**, □) and yields of cyclohexanone oxime (**2**, ○), cyclohexylamine (**3**, △), cyclohexanone (**4**, ▲), cyclohexyl-cyclohexylidene amine (**5**, ×), and dicyclohexylamine (**6**, ●) vs. time for the hydrogenation of nitrocyclohexane at 100 °C with (A) Au/Al-2.5, (B) Au/Ti-3.6, and (C) Pt/Al-1.3.



Scheme 1. Possible reaction scheme for the hydrogenation of nitrocyclohexane with H₂.

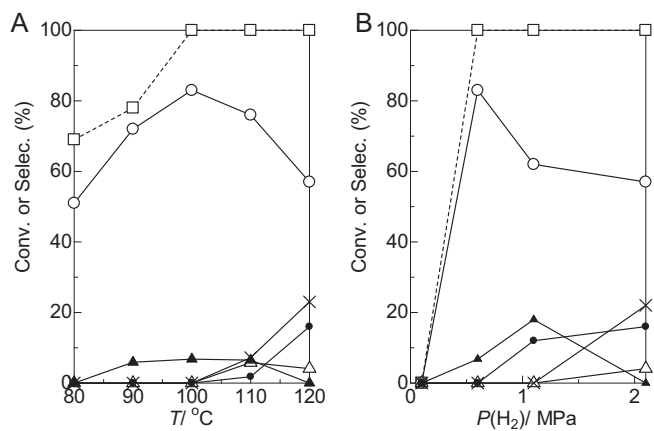


Fig. 2. Effects of (A) temperature and (B) hydrogen pressure on the conversion of nitrocyclohexane (1, □) and yields of cyclohexanone oxime (2, ○), cyclohexylamine (3, △), cyclohexanone (4, ▲), cyclohexyl-cyclohexylidene amine (5, ×), and dicyclohexylamine (6, ●) for the hydrogenation of nitrocyclohexane with Au/Al-2.5. Conditions: (A) $t = 6$ h, $P(\text{H}_2) = 0.6$ MPa; (B) $T = 100$ °C, $t = 6$ h.

$P(\text{H}_2) = 0.6$ MPa), the cyclohexanone oxime yield of 83% with 6.8% yield of cyclohexanone (4) as byproduct. The cyclohexanone oxime yield is comparable to that of Na-doped Pt/TiO₂ catalyst [18]. It should be noted that Au/Al-2.5, as an additive-free non-platinum metal catalyst, achieved selective hydrogenation of nitrocyclohexane to cyclohexanone oxime.

3.2. Size- and support-dependent activity of Au NPs

For a series of Au/Al catalysts with the same Au loading (1 wt%) but with different gold particle size, the conversion and the selectivity to cyclohexanone oxime are plotted as a function of the average particle size in Fig. 3. Clearly, the Au clusters with the smallest size (2.5 nm) gave highest conversion. The increase of Au particle size from 2.5 nm to 6.0 nm results in a drastic decrease in the conversion (from 100% to 4.5%) and the selectivity to cyclohexanone oxime (from 83% to 0%). It is clearly shown that the present reaction requires small Au clusters.

The activity of the gold clusters having similar mean size (1.9–3.6 nm) depends strongly on the acid–base characteristics of support material. In Fig. 4, conversion of nitrocyclohexane and yield of cyclohexanone oxime are plotted as a function of the electronegativity of metal oxide which has been used, to a first approximation,

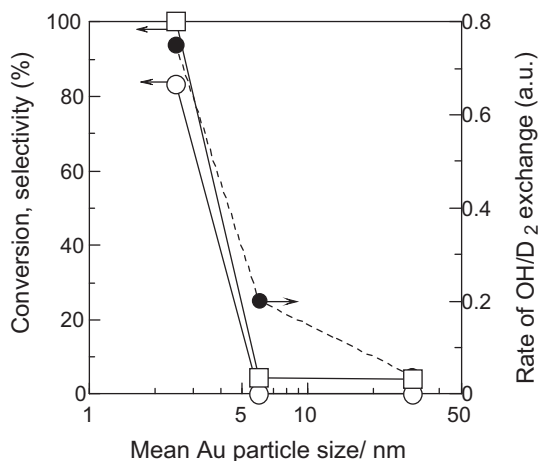


Fig. 3. (□) Conversion of nitrocyclohexane and (○) cyclohexanone oxime selectivity for nitrocyclohexane hydrogenation at 100 °C and (●) initial rates of OH/D₂ isotope exchange as a function of average particle size of Au in Au/Al.

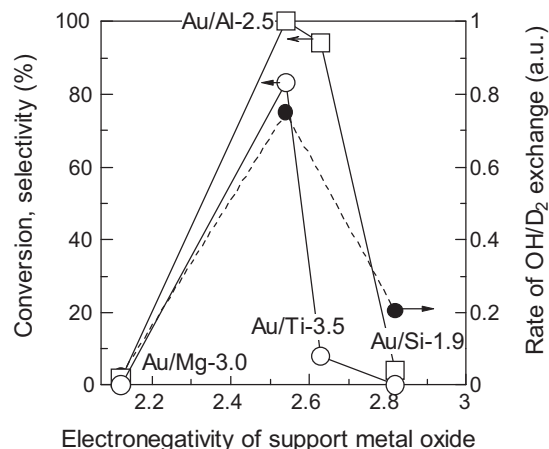


Fig. 4. (□) Conversion of nitrocyclohexane and (○) cyclohexanone oxime selectivity for nitrocyclohexane hydrogenation at 100 °C and (●) initial rates of OH/D₂ isotope exchange as a function of electronegativity of support oxide.

as a parameter of acidity (or electrophilicity) of metal oxides [9]. The result shows that the support with strong basic character (MgO) and that with acidic character (SiO₂) resulted in lower activity and selectivity than an amphoteric oxide, Al₂O₃. This result suggests that both acidic and basic sites of the support material are necessary for this reaction.

3.3. Roles of Au cluster and Al₂O₃

Previously, Claus et al. reported the isotopic exchange of OH groups of oxide supports to OD groups in D₂ for Ag/SiO₂ catalyst [22]. They showed that the reaction begins with the cleavage of D₂. In our previous study [9], we carried out in situ IR experiments for the isotopic exchange of M–OH to M–OD under D₂ on metal oxides (MO_x)-supported Au catalysts, and the rate of OH/D₂ exchange was used to compare the relative rate of H₂ dissociation on various Au catalysts. As shown in Fig. 5, the initial rates of OD formation ($\Delta A_{\text{OD}}/\Delta t$) on Au/Al-2.5, estimated from the slope of the curve, was significantly higher than that for γ -Al₂O₃, which indicates that the Au cluster plays a significant role in the cleavage of a H–H bond. To obtain mechanistic reasons of the size- and support-dependent activity of gold catalyst, the OD formation rate reported in our previous study [9] is plotted in Figs. 3 and 4. For Au/Al catalysts with the same Au loading but with different mean Au particle sizes, the rate of OD formation decreased with increase in the Au particle size. This trend is

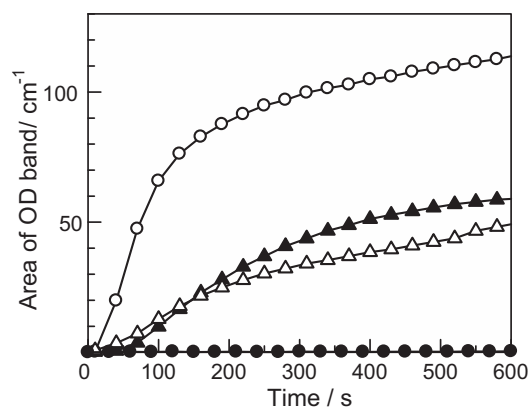


Fig. 5. Area of OD band as a function of the time of D₂ exposure at 150 °C to (○) untreated Au/Al-2.5, (▲) pyridine-adsorbed Au/Al-2.5, (△) CH₃COOH-adsorbed Au/Al-2.5, and (●) γ -Al₂O₃.

Table 2
Effect of additives (20 mol%) on Au/Al-2.5 catalyzed hydrogenation of nitrocyclohexane^a and nitrobenzene.^b

Additive	$\Delta A_{OD}/\Delta t^c$ (cm ⁻¹ s ⁻¹)	[PhNO ₂ ad] ^d (cm ⁻¹)	1 Conv. (%)	2 Sel. (%)	Yield (%)					Yield (%)
					2	3	4	5	6	
–	0.73	18.1	100	83	83	0	6.8	0	0	94
Pyridine	0.14	6.0	77	54	42	2.4	5.2	0	2.4	31
CH ₃ COOH	0.12	2.6	26	65	17	0	5.0	0	0	53

^a Nitrocyclohexane (0.5 mmol), EtOH (1.5 mL), Au/Al-2.5 (0.25 mol%), $t = 6$ h, $P(\text{H}_2) = 0.6$ MPa, $T = 100$ °C.

^b Nitrobenzene (3 mmol) in EtOH (1.5 mL) with Au/Al-2.5 (0.1 mol%): $t = 2$ h, $P(\text{H}_2) = 2.0$ MPa, $T = 110$ °C. Yield of aniline was determined by GC.

^c The initial rates of OD formation under D₂ flow (from Fig. 5).

^d The relative amount of adsorbed nitrobenzene at 100 °C estimated from integrated intensity of the $\nu_s(\text{NO}_2)$ band (1350 cm⁻¹) of the adsorbed nitrobenzene in Fig. 6.

consistent with the changes in the activity and selectivity for the selective hydrogenation (Fig. 3). Taking into account the fact that dissociative chemisorption of H₂ on the extended surface of polycrystalline or single crystal gold surface is thermodynamically unfavorable, coordinatively unsaturated sites on small Au clusters are responsible for the H₂ dissociation as a possible rate-limiting step for the title reaction. As for the support effect, the OH/D₂ exchange reaction rate for acid–base bifunctional support (Al₂O₃) is higher than those for basic (MgO) and acidic (SiO₂) supports, and this trend is consistent with the changes in the activity and selectivity for the selective hydrogenation (Fig. 4). This indicates that the surface acid–base pair sites on the support are also required for the H₂ dissociation step.

To further investigate the role of the Al₂O₃ surface, the effects of basic or acidic additives to the reaction mixture were examined. Table 2 shows the catalytic results for the Au/Al-2.5 catalyzed hydrogenation of nitrocyclohexane in the absence or presence of 20 mol% of pyridine or acetic acid. The addition of these molecules decreased the conversion and the selectivity to cyclohexanone oxime. The yield of cyclohexanone oxime in the presence of pyridine and acetic acid was ca. 1/2 and 1/5 of the value in the additive-free condition. The additive effects were also studied for the hydrogenation of nitrobenzene as a test reaction. The addition of pyridine and acetic acid decreased the aniline yield. As shown in Fig. 5, the rate of OH/D₂ exchange reaction after the pre-adsorption of pyridine (0.6 mmol/g) was ca. 1/5 of the value in the additive-free condition. The pre-adsorption of acetic acid (0.6 mmol/g) also resulted in a decrease in the rate of OH/D₂ exchange reaction by a factor of 1/6. These results suggest that Lewis acid–base pair sites also play an important role in H₂ dissociation and subsequent formation of acidic Al–OH group. Most probable model to account for the above results is that the dissociation of H₂ occurs at gold cluster–support interface [23], where coordinatively unsaturated Au atoms and the acid–base pair site (Al^{δ+}–O^{δ-} site) are located close to each other. Recently, Garcia and co-workers showed direct IR evidences on heterolytic dissociation of H₂ on ceria-supported Au NPs at 150 °C, leading to a proton bonded to a ceria oxygen and a hydride bonded to gold [24]. For the chemoselective hydrogenation of polar bonds (C=O or C=N) with homogeneous metal–ligand bifunctional catalysts, it is widely accepted that the reaction begins with heterolytic cleavage of H₂ to yield H⁺ in an OH or NH ligand and H⁻ in metal hydrides, and the H⁺/H⁻ pair preferentially transfers to the polar bonds [25,26]. On the other hand, it is established that H₂ addition to metal particles on solid acids, such as Pt/SO₄²⁻–ZrO₂, Pt/Al₂O₃, and Rh/Al₂O₃, results in the formation of acidic OH groups on the support via hydrogen spillover [27]. Adopting these models, a cooperative mechanism catalyzed by low coordinated Au atoms and acid–base pair site of Al₂O₃ for the hydrogenation of a nitro group may be proposed as follows. The dissociation of H₂ at gold–support interface yields an H^{δ-} atom on the low coordinated Au atom and an H atom which releases an electron to Lewis acid site of the support. The latter species becomes a proton stabilized at the oxygen atom (Lewis base) nearby the Lewis acid site. The electrophilic H^{δ+} species on the support and

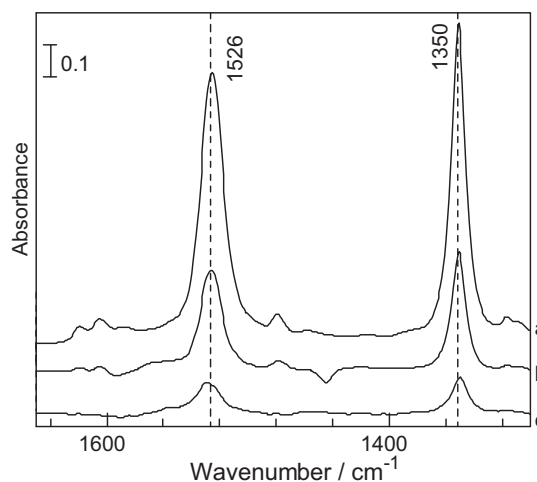


Fig. 6. IR spectra of the adsorbed nitrobenzene at 100 °C on (a) untreated Au/Al-2.5, (b) pyridine-adsorbed Au/Al-2.5, and (c) CH₃COOH-adsorbed Au/Al-2.5.

nucleophilic H^{δ-} species on Au atom transfer to the polar nitro group.

For the selective hydrogenation of nitrocyclohexane on the Na-doped Pt/TiO₂ catalyst, Serna et al. [18] proposed that the preferential adsorption of the nitro group on Pt–TiO₂ interface is the origin of the selective production of cyclohexanone oxime. To study a possible role of acid–base pair sites on Al₂O₃ in preferential adsorption of the nitro group, in situ FTIR experiments of nitrobenzene adsorption on Au/Al-2.5 was carried out. Note that the IR spectrum of adsorbed nitrocyclohexane was complicated, and hence nitrobenzene was used as probe molecule. When nitrobenzene was adsorbed on Au/Al-2.5 at 100 °C (Fig. 6), IR bands due to the $\nu_{as}(\text{NO}_2)$ and $\nu_s(\text{NO}_2)$ of the adsorbed nitrobenzene were observed at 1525 and 1350 cm⁻¹, respectively. In our previous study, the $\nu_{as}(\text{NO}_2)$ band with lower frequency than gas phase PhNO₂ (1552 cm⁻¹) has been assigned to nitrobenzene ad-species interacting with the Al₂O₃ surface through the nitro group [9]. The pre-adsorption of pyridine and acetic acid decreased the intensity of these bands; the relative amounts of adsorbed nitrobenzene on Au/Al-2.5, estimated from the integrated area of the band at 1350 cm⁻¹, were 1/3 and 1/7 of the value in the additive-free condition. Taking into account the fact that the adsorption of acetic acid on Al₂O₃ results in the formation of the acetate ion the acid–base pair site (Al^{δ+}–O^{δ-} site) [28], the result indicates the preferential adsorption of the nitro group on Al^{δ+}–O^{δ-} site. This can be additional reason why alumina is the most effective support material for the gold catalyzed selective hydrogenation of nitro-compounds.

4. Conclusion

We demonstrated that highly selective reduction of nitrocyclohexane into cyclohexanone oxime is effectively catalyzed by γ -Al₂O₃-supported Au cluster catalyst, prepared by colloid depo-

sition method. The activity depended strongly on the size and support oxides, and small Au clusters (2.5 nm) on the acid–base bifunctional support (Al_2O_3) gave highest activity and selectivity. We propose a possible mechanism that account for these observations; at gold cluster–support interface, cooperation of coordinatively unsaturated Au atoms and the acid–base pair site of alumina ($\text{Al}^{\delta+}-\text{O}^{\delta-}$ site) plays an important role in the dissociation of H_2 as a possible rate-limiting step. The preferential adsorption of the nitro group on $\text{Al}^{\delta+}-\text{O}^{\delta-}$ site can be additional reason of high activity and selectivity.

Acknowledgments

This work was supported by the Japanese Ministry of Education, Culture, Sports, Science and Technology (Grant-in-Aids for Scientific Research B 20360361 and for Young Scientists A 22686075) and JST (Adaptable and Seamless Technology Transfer Program through Target-driven R&D).

References

- [1] M. Haruta, *Catal. Today* 36 (1997) 153–166.
- [2] A. Corma, H. Garcia, *Chem. Soc. Rev.* 37 (2008) 2096–2126.
- [3] M.M. Schubert, S. Hackenberg, A.C. van Veen, M. Muhler, V. Plzak, R.J. Behm, *J. Catal.* 197 (2001) 113–122.
- [4] P. Claus, A. Brückner, C. Mohr, H. Hofmeister, *J. Am. Chem. Soc.* 122 (2000) 11430–11439.
- [5] C.K. Costello, J. Guzman, J.H. Yang, Y.M. Wang, M.C. Kung, B.C. Gates, H.H. Kung, *J. Phys. Chem. B* 108 (2004) 12529–12536.
- [6] T. Ishida, N. Kinoshita, H. Okatsu, T. Akita, T. Takei, M. Haruta, *Angew. Chem. Int. Ed.* 47 (2008) 9265–9268.
- [7] A. Corma, P. Serna, H. Garcia, *J. Am. Chem. Soc.* 129 (2007) 6358–6359.
- [8] Y. Tai, M. Watanabe, K. Kaneko, S. Tanemura, T. Miki, J. Murakami, K. Tajiri, *Adv. Mater.* 13 (2001) 1611–1614.
- [9] K. Shimizu, Y. Miyamoto, T. Kawasaki, T. Tanji, Y. Tai, A. Satsuma, *J. Phys. Chem. C* 113 (2009) 17803–17810.
- [10] M. Okumura, Y. Kitagawa, M. Haruta, K. Yamaguchi, *Appl. Catal. A* 291 (2005) 37–44.
- [11] A. Corma, M. Boronat, S. Gonzalez, F. Illas, *Chem. Commun.* (2007) 3371–3373.
- [12] E. Bus, J.T. Miller, J.A. van Bokhoven, *J. Phys. Chem. B* 109 (2005) 14581–14587.
- [13] J.A. van Bokhoven, J.T. Miller, *J. Phys. Chem. C* 111 (2007) 9245–9249.
- [14] T. Tatsumi, N. Jappar, *J. Catal.* 161 (1996) 570–576.
- [15] J.A. Robertson, *J. Org. Chem.* 13 (1948) 395–398.
- [16] GB Patent 857902 (1958), to DuPont.
- [17] J.F. Knifton, *J. Catal.* 33 (1974) 289–298.
- [18] P. Serna, M. Lopez-Haro, J.J. Calvino, A. Corma, *J. Catal.* 263 (2009) 328–334.
- [19] S. Sakaguchi, Y. Nishiwaki, T. Kitamura, Y. Ishii, *Angew. Chem. Int. Ed.* 40 (2001) 222–224.
- [20] K. Yamaguchi, S. Shinachi, N. Mizuno, *Chem. Commun.* (2004) 424–425.
- [21] M. Brust, M. Walker, D. Bethell, D.J. Schiffrin, R. Whyman, *J. Chem. Soc. Chem. Commun.* (1994) 801–802.
- [22] M. Bron, D. Teschner, A. Knop-Gericke, F.C. Jentoft, J. Krohnert, J. Hohmeyer, C. Volckmar, B. Steinhauer, R. Schlögl, P. Claus, *Phys. Chem. Chem. Phys.* 9 (2007) 3559–3569.
- [23] T. Fujitani, I. Nakamura, T. Akita, M. Okumura, M. Haruta, *Angew. Chem. Int. Ed.* 48 (2009) 9515–9518.
- [24] R. Juárez, S.F. Parker, P. Concepción, A. Corma, H. García, *Chem. Sci.* 1 (2010) 731–738.
- [25] R. Noyori, T. Ohkuma, *Angew. Chem. Int. Ed.* (2001) 40–73, 40–73.
- [26] R.M. Bullock, *Chem. Eur. J.* 10 (2004) 2366–2374.
- [27] T. Shishido, H. Hattori, *Appl. Catal. A* 146 (1996) 157–164.
- [28] K. Shimizu, H. Kawabata, A. Satsuma, T. Hattori, *J. Phys. Chem. B* 103 (1999) 5240–5245.